

Molecular Structure and Dynamics in Thin Water Films at the Silica and Graphite Surfaces

Dimitrios Argyris, Naga Rajesh Tummala, Alberto Striolo, and David R. Cole

J. Phys. Chem. C, **2008**, 112 (35), 13587-13599 • DOI: 10.1021/jp803234a • Publication Date (Web): 29 July 2008

Downloaded from <http://pubs.acs.org> on April 5, 2009

More About This Article

Additional resources and features associated with this article are available within the HTML version:

- Supporting Information
- Access to high resolution figures
- Links to articles and content related to this article
- Copyright permission to reproduce figures and/or text from this article

[View the Full Text HTML](#)

Molecular Structure and Dynamics in Thin Water Films at the Silica and Graphite Surfaces

Dimitrios Argyris, Naga Rajesh Tummala, and Alberto Striolo*

*The University of Oklahoma, School of Chemical, Biological, and Materials Engineering,
Norman, Oklahoma 73019*

David R. Cole

*Oak Ridge National Laboratory, Aqueous Chemistry and Geochemistry Group, Chemical Sciences Division,
Oak Ridge, Tennessee 37831-6110*

Received: April 14, 2008; Revised Manuscript Received: May 28, 2008

The structure and dynamic properties of interfacial water at the graphite and silica solid surfaces were investigated using molecular dynamics simulations. The effect of surface properties on the characteristics of interfacial water was quantified by computing density profiles, radial distribution functions, surface density distributions, orientation order parameters, and residence and reorientation correlation functions. In brief, our results show that the surface roughness, chemical heterogeneity, and surface heterogeneous charge distribution affect the structural and dynamic properties of the interfacial water molecules, as well as their rate of exchange with bulk water. Most importantly, our results indicate the formation of two distinct water layers at the SiO₂ surface covered by a large density of hydroxyl groups. Further analysis of the data suggests a highly confined first layer where the water molecules assume preferential hydrogen-down orientation and a second layer whose behavior and characteristics are highly dependent on those of the first layer through a well-organized hydrogen bond network. The results suggest that water–water interactions, in particular hydrogen bonds, may be largely responsible for macroscopic interfacial properties such as adsorption and contact angle.

1. Introduction

Water at interfaces has generated, and continues to generate, significant research interest especially at nanoscale dimensions where unexpected chemical and physical phenomena may appear. The study of interfacial water has potential impact in many different fields ranging from geology,^{1,2} nanotribology,^{3–5} microfluidics,⁶ laboratory-on-a-chip, and molecular engineering.^{7,8} Structural properties of interfacial water are of significant importance in biological systems⁹ and various specific processes such as the structure–function relationship of ion channels,^{10–12} the dynamic behavior of biological membranes,^{13,14} and biolubrication. Understanding the structure and behavior of water near different substrates can clarify a number of phenomena and processes, typically classified as hydrophobic and hydrophilic effects.

Experimental studies have elucidated several features about structural and dynamic properties of water in contact with various hydrophobic and hydrophilic systems.^{5,13,15–17} Commonly, simulations have contributed to a better understanding and interpretation of experimental results.¹⁶ Both molecular dynamics and Monte Carlo simulation techniques have been employed to study interfacial water on surfaces such as silicon and graphite.^{16,18–27} A well established conclusion is that both structural and dynamic properties of interfacial water depend on the atomic-scale geometry and heterogeneous chemical properties of the solid substrate. Computer simulation studies have also addressed the structural properties of water inside and outside carbon nanotubes and around fullerenes.^{28–32}

Despite this wealth of research, a number of key issues remain unresolved. For instance, it is not clear how the solid structure

perturbs interfacial water and how far from the solid this perturbation persists.³³ Important dynamic properties such as the rate of water reorientation and exchange in the perturbed layer need to be investigated further. It is also of interest to identify the structural properties (e.g., atomic scale roughness and/or heterogeneous distribution of partially charged groups on the solid surface) that render a substrate hydrophobic and hydrophilic as determined from macroscopic observation (e.g., contact angle measurements). One possible route to answer this scientific question is to conduct simulations of thin water films on a number of well controlled surfaces with different degrees of hydrophilicity. Then, by analyzing how the structural and dynamic properties of the interfacial water molecules change as the substrate goes from hydrophobic to hydrophilic, it is possible to provide a bridge between the atomic-scale properties of a solid surface and the macroscopic observations. This is the purpose of the present work. Our main objective is to investigate the structure and dynamics of water molecules and the hydrogen bonding network that develops when water molecules interact with a solid crystalline substrate. This study focuses on the properties of water within the first few molecular layers from the substrate, where significant structural and dynamic changes are observed compared to bulk properties. A detailed layer-by-layer analysis is provided below for structural and dynamic properties and how they depend on the solid substrates.

This manuscript is organized as follows. In section 2, we provide simulation details and algorithms, in section 3, we discuss our main results, and in section 4, we summarize our conclusions.

* To whom correspondence should be addressed. E-mail: astriolo@ou.edu. Phone: 405 325 5716. Fax: 405 325 5813.

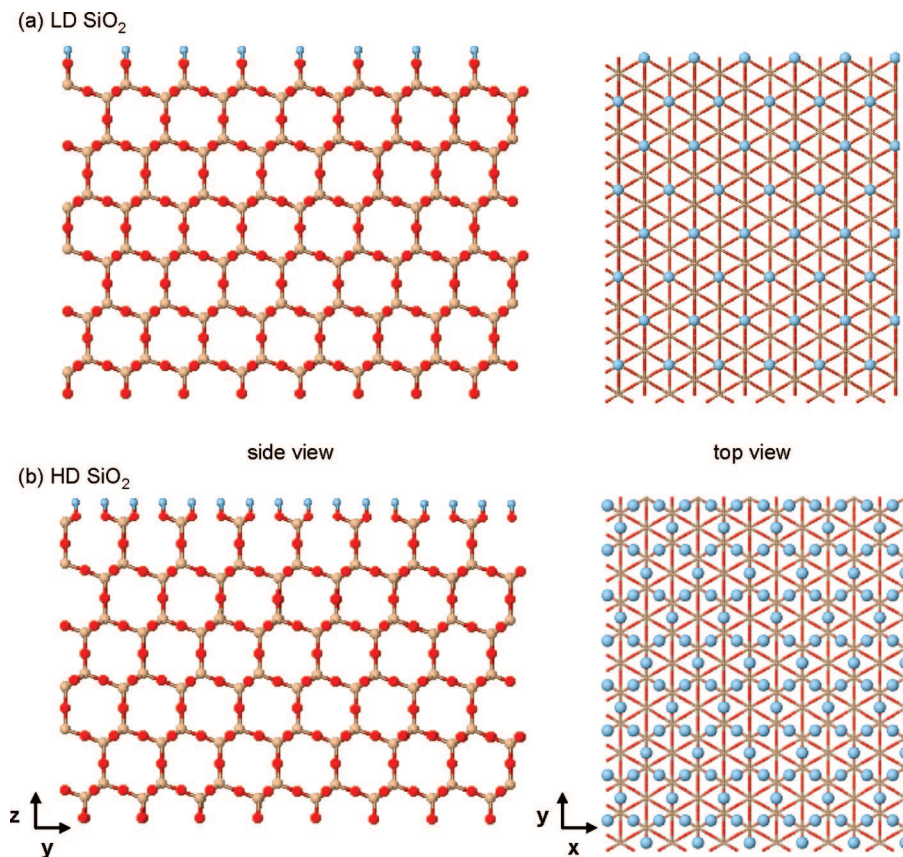


Figure 1. Side and top views of LD SiO₂ (a) and HD SiO₂ (b) surfaces. Blue, red, and tan spheres represent the hydrogen atoms of the surface hydroxyl groups and oxygen and silicon atoms, respectively.

2. Simulation Methodology and Details

The goal of this study is to investigate the behavior and structural properties of a thin water film in contact with three solid surfaces. The surfaces are chosen to represent different degrees of hydrophilicity. The first surface considered is graphite, which is composed of three graphene sheets separated by 3.35 Å from each other. The solid substrates are aligned parallel to the *x* and *y* plane. Simulations were carried out in orthorhombic simulation boxes of constant volume. The *x* and *y* dimensions of the simulation boxes reflect the periodicity of the solid crystalline substrate. In the case of graphite, the *x* and *y* dimensions are 29.5 and 34.1 Å, respectively. The second and third surfaces were obtained from the crystal structure of β -cristobalite SiO₂.³⁴ To obtain a realistic surface structure, we followed the procedure of Pellenq and co-workers.¹⁸ The crystal was cut along the (1 1 1) crystallographic face. All of the silicon atoms that are part of an incomplete tetrahedral were removed and the nonbridging oxygen atoms (bonded to only one silicon atom) were saturated with hydrogen atoms. The hydrogen atoms were positioned 1 Å perpendicular to the surface and treated as rigid. By cutting the cristobalite crystal at different depths, we obtained two surfaces with different hydroxyl surface density and thus different degrees of hydrophobicity. The two surfaces are identified as low hydroxyl surface density (LD), with 4.54 OH/nm², and high hydroxyl surface density (HD) with 13.63 OH/nm². Albeit these models represent approximations of solid surfaces, they allow us to understand how the thermodynamic and structural properties of interfacial water depend on the presence, density, and orientation of hydroxyl groups on the solid substrate. In the case of silica surfaces, the *x* and *y* simulation box dimensions are 30.2 and 34.9 Å, respectively. The solid slab thickness is 25.7 Å for the LD silica surface and

23.6 Å for the HD one. A thicker solid slab for the silica surfaces, compared to graphite, was considered because the electrostatic interactions are significant in these substrates. Top views of the silica surfaces are shown in Figure 1 where the surface hydroxyl groups can be seen.

Two identical faces of the same rigid substrate were considered facing each other to represent a slit-shaped pore. Water was allowed in the space between the two solid surfaces. The simulation box was built by placing one slab of the solid substrates at the base and another, specularly symmetric, at a distance $H = 140$ Å along the *z* axis. To minimize interactions between the images of molecules along the *z* direction, an additional vacuum of thickness 30 Å was considered in the outermost side of the pores. The number of water molecules was 1000, and it was kept fixed, except when otherwise noted. Water molecules were placed in between the solid substrates as shown in Figure 2 for the case of graphite. Periodic boundary conditions were applied along the *x*, *y*, and *z* axes.

The water molecules were simulated using the simple point charge/extended (SPC/E) model.³⁵ Carbon atoms of the graphite were held stationary and modeled as Lennard-Jones (LJ) spheres employing the parameters proposed by Chang and Steele.³⁶ The atoms of the silica substrates interact with water molecules by means of dispersive and electrostatic forces.³⁷ The dispersive interactions were modeled with a 12–6 Lennard-Jones potential. The LJ parameters for unlike interactions were determined using the Lorentz–Berthelot mixing rules.³⁸ The cutoff distance for all interactions was set to 9 Å, and the long-range electrostatic interactions were treated using the Ewald summation method.³⁸ Bond lengths and angles in water molecules were kept fixed using the SHAKE algorithm.³⁹ In Table 1, we report all of the parameters used to represent the force field in our simulations.

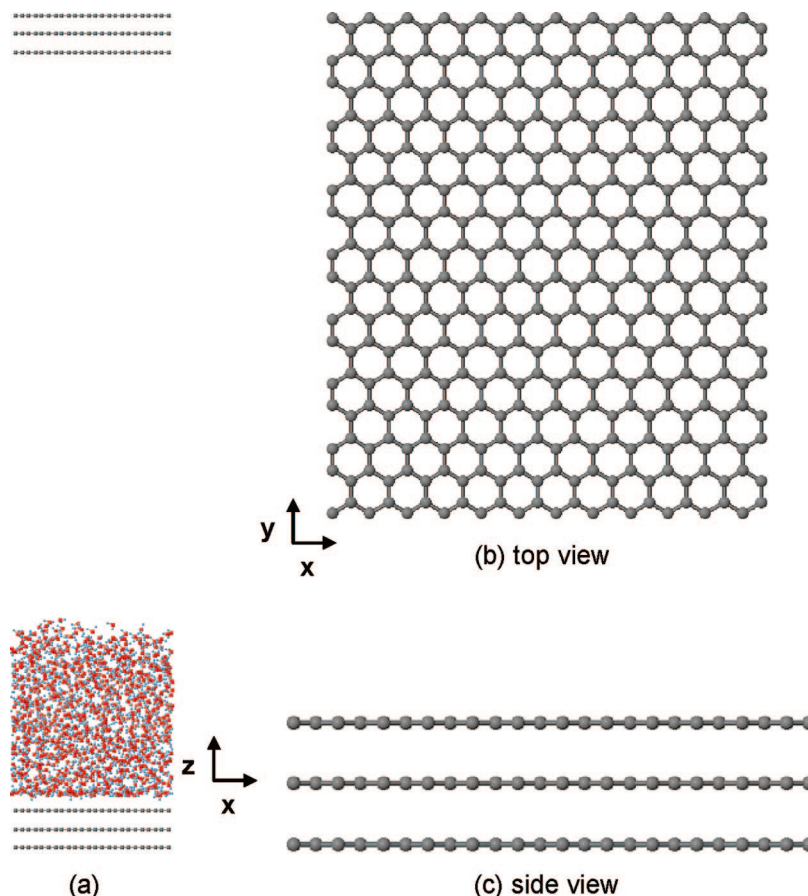


Figure 2. Snapshots of the graphite substrates used in our simulations. (a) Side view of the entire simulation box with water molecules in contact with the lower graphite surface. (b) Top and (c) side view of the graphite surface. In the top view, only one of the graphene sheets is shown for clarity.

TABLE 1: Parameters Used within the Force Fields Implemented in Our Simulations^a

	site	σ (Å)	ϵ (kcal/mol)	q (e)
water	O	3.166	0.155402	-0.8476
	H	0.000	0.000000	0.4238
graphite	C	3.400	0.055700	0.0000
	Si	0.000	0.000000	1.2830
silica	bO	2.700	0.456757	-0.6290
	nbO	3.000	0.456757	-0.5330
	H	0.000	0.000000	0.2060

^aIn the case of silica, bO and nbO stand for bridging and non-bridging oxygen atoms, respectively.

Note that silicon atoms do not interact via dispersive interactions with water molecules.

The simulations were conducted using the large-scale atomic/molecular massively parallel simulator (LAMMPS).⁴⁰ All simulations were performed in the canonical ensemble (NVT) where the number of particles (N), the simulation box volume (V), and the temperature (T) were kept constant. The system temperature was set at 300 K and controlled by a Nosé-Hoover thermostat with a relaxation time of 100 fs. The integration of the equations of motion was performed by the velocity-Verlet algorithm³⁸ with a time step of 1 fs. Each simulation ran for 10^6 time steps that accounts for 1 ns of total simulation time. All of the results presented in this study were obtained after 0.2 ns of equilibration time. During the production time, which lasted 0.8 ns, the atom positions were recorded every 200 time steps, corresponding to 0.2 ps, and retained for further analysis.

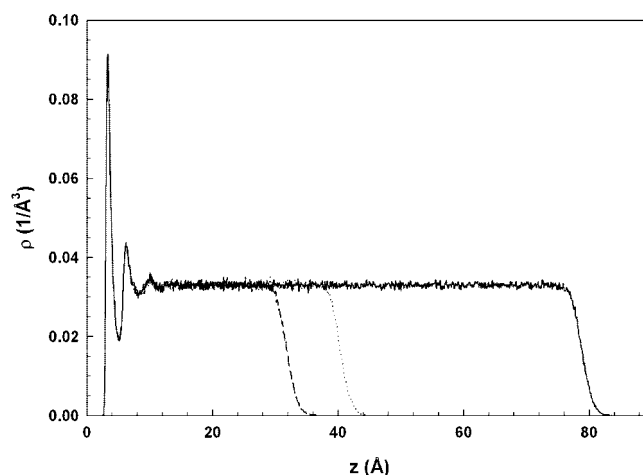


Figure 3. Oxygen atomic density as a function of distance z from the graphite surface. The oxygen atoms are those of water molecules. Three cases are shown in which 2592 (solid line), 1296 (dotted line), and 1008 (dashed line) water molecules were simulated. In all cases $T=300$ K.

3. Results

3.A. Structural Properties: Atom Density Profiles. To assess the effect of film thickness on all properties of interfacial water molecules we conducted a number of simulations where the number of water molecules was reduced from 2592 to 1008. The results are shown in Figure 3 in terms of atomic density profiles of the oxygen atom of water molecules as a function of the distance from the graphite surface. As expected, the film

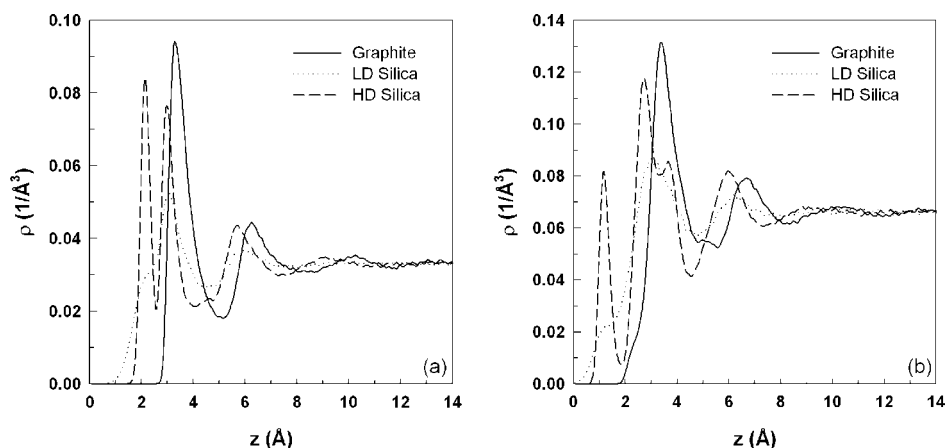


Figure 4. (a) Oxygen and (b) hydrogen atom density profiles as a function of distance z from the solid surfaces. The reference $z=0$ is the top plane of carbon atoms in the case of the graphite surface and the plane of nonbridging oxygen atoms in the case of both LD and HD silica surfaces.

TABLE 2: Location (Expressed at Distance z from the Surface) of the Atomic Density Peaks of Oxygen and Hydrogen Atoms on the Various Surfaces Considered in Figure 4^a

surface	oxygen peak (Å)	hydrogen peak (Å)	layer label
graphite (A)	3.25	3.35	AO-1/AH-1
	6.25	6.65	AO-2/AH-2
LD SiO ₂ (B)	2.15	1.15	BO-1/BH-1 ^b
	3.05	2.95	BO-2/BH-2
	6.00	6.25	BO-3/BH-3
HD SiO ₂ (C)	2.15	1.15	CO-1/CH-1
	2.95	2.75	CO-2/CH-2
	5.75	3.65	CO-3/CH-3
		6.05	CO-4/CH-4

^aOn the fourth column we provide the labels used in our discussion to refer to the peaks. The first and second letters of the labels indicate the substrate and the atomic species, respectively. The number in the label corresponds to the layer, layer 1 being the one closer to the substrate. ^bThis position corresponds to a ‘‘shoulder’’ in the density profile.

thickness decreases as the number of simulated water molecules decreases, but our results indicate that the density profiles at the graphite–water interface, as well as that at the water–vacuum interface, do not depend on the film thickness. Further, the density profile at the center of the thin film is similar in all the cases considered. Thus, for economy of computational time we focused on thin films of 1000 water molecules at the solid–liquid interface in the remainder of this work.

In Figure 4 we show plots of the atomic densities of oxygen and hydrogen atoms of water molecules as a function of the distance z perpendicular to the surfaces. Results are shown when the solid surface is graphite (solid line), LD SiO₂ (dotted line), and HD SiO₂ (dashed line). The reference point ($z = 0$) for the density profile is the center of carbon atom in the outermost graphene sheet in the case of graphite and that of the nonbridging oxygen atoms in the LD or HD SiO₂ surfaces. The location of all the peaks that are observed in the density profiles in Figure 4 are reported and labeled in Table 2. This labeling will become useful in the following discussion. In the case of water on graphite (continuous line), the results presented in figure 4a indicate one pronounced peak at 3.25 Å that clearly signifies the formation of one layer of water molecules. In the same plot a second, less pronounced peak can be detected at 6.25 Å. In the case of the LD SiO₂ substrate, a distinct peak is located at 3.05 Å and a second, less pronounced peak appears at approximately 6.00 Å. Further, the appearance of a ‘‘shoulder’’ at 2.15 Å indicates the presence of structured water molecules very

close to the LD SiO₂ surface. Interestingly, two pronounced layers of oxygen atoms are manifested at 2.15 and 2.95 Å on the HD SiO₂ surface. This suggests that a large amount of water molecules accumulate closer to the surface because of the increased surface hydroxyl density. In particular, we observe that the ‘‘shoulder’’ that appears at 2.15 Å on LD SiO₂ surface becomes a fully developed peak on the HD SiO₂. On the latter surface a smaller peak develops at 5.75 Å, closer to the surface than the peak at ~6.00 Å observed on the LD SiO₂ surface.

Commensurate with the structuring of water evident from the oxygen atomic density profiles, in Figure 4b we observe layers of water hydrogen atoms. The most interesting data are those obtained on the HD SiO₂ surface. In this case (dashed line), four layers of hydrogen atoms appear at 1.15, 2.75, 3.65 and 6.05 Å. Consideration of the first peak (at 1.15 Å) on the HD SiO₂ surface in Figure 4b combined with the corresponding oxygen atoms located 1 Å above (the peak at 2.15 Å in Figure 4a) suggests a hydrogen-down orientation of the water molecules. Further, the highest peak (at 2.75 Å) on the HD SiO₂ in Figure 4b corresponds to the layer of hydrogen atoms that could belong to the water molecules of the first (at 2.15 Å) or second (at 2.95 Å) layer observed in the oxygen atomic density profiles in Figure 4a. Similarly to what observed for the oxygen atomic density profiles, we noticed that the first peak that appears in the hydrogen density profile at 1.15 Å at the HD SiO₂ is only a shoulder on the LD SiO₂ surface. This indicates that increasing the surface density of hydroxyl groups has a very pronounced effect on the structure of interfacial water.

3.B. Structural Properties: In-Plane Radial Distribution Functions. The results in Figure 4 clearly indicate that the presence of solid surfaces affect the density of the interfacial water, with the formation of layers of different density. This is in agreement with the work presented by a number of other groups.^{16,18,23,41} It is now of interest to determine whether or not water molecules belonging to each layer show pronounced differences when compared to the bulk. The results presented in Figure 5, Figure 6, and Figure 7 show in-plane oxygen–oxygen, $g_{OO}(r)$, hydrogen–hydrogen, $g_{HH}(r)$, and oxygen–hydrogen, $g_{OH}(r)$ radial distribution functions (RDFs). The RDFs are calculated in correspondence of slabs at several distances from the surface. The thickness (δz) of the slab is 1 Å in all cases and the center of a slab corresponds to the peak of one specific layer as reported in Table 2. In some cases the center of the slab had to be displaced by 0.1 to 0.2 Å from the peak position in order to avoid interferences from atoms of adjacent layers. The in-plane RDFs obtained in correspondence to the interfacial

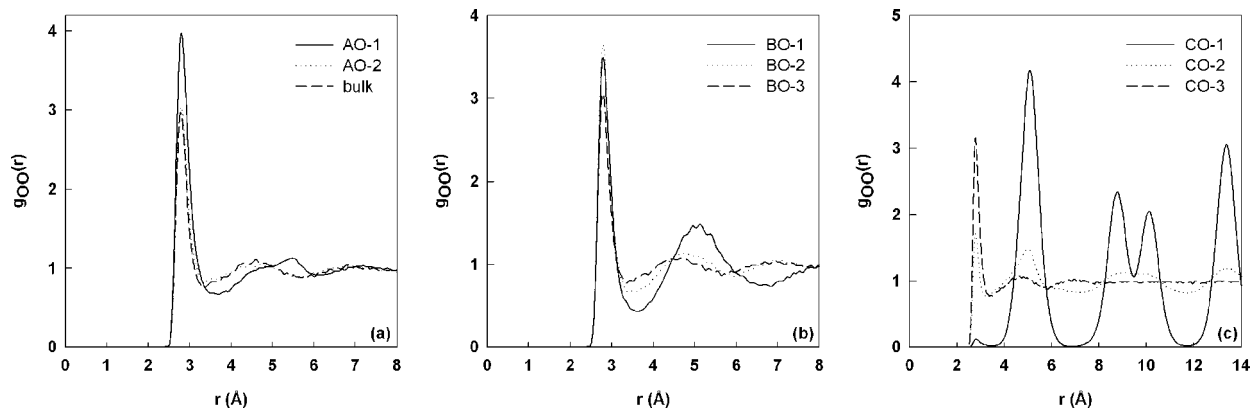


Figure 5. In-plane oxygen–oxygen radial distribution functions $g_{OO}(r)$ on graphite (a), LD SiO₂ (b), and HD SiO₂ (c). The dashed line of figure (a) corresponds to a in-plane RDF far from the surfaces ($z > 14\text{Å}$) and is identical in all cases.

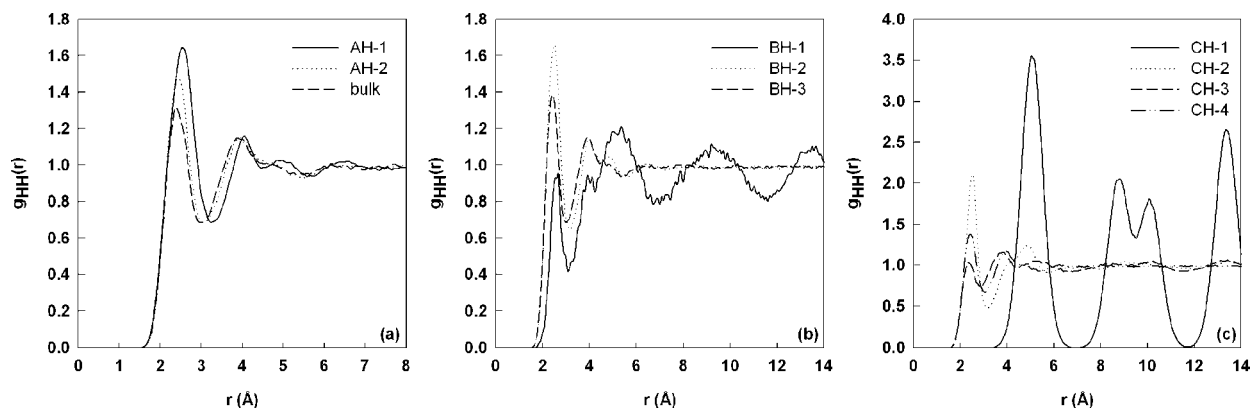


Figure 6. In-plane hydrogen–hydrogen radial distribution functions $g_{HH}(r)$ on graphite (a), LD SiO₂ (b), and HD LD SiO₂ (c). The dashed line of figure (a) corresponds to a in-plane RDF far from the surfaces ($z > 14\text{Å}$) and is identical in all cases.

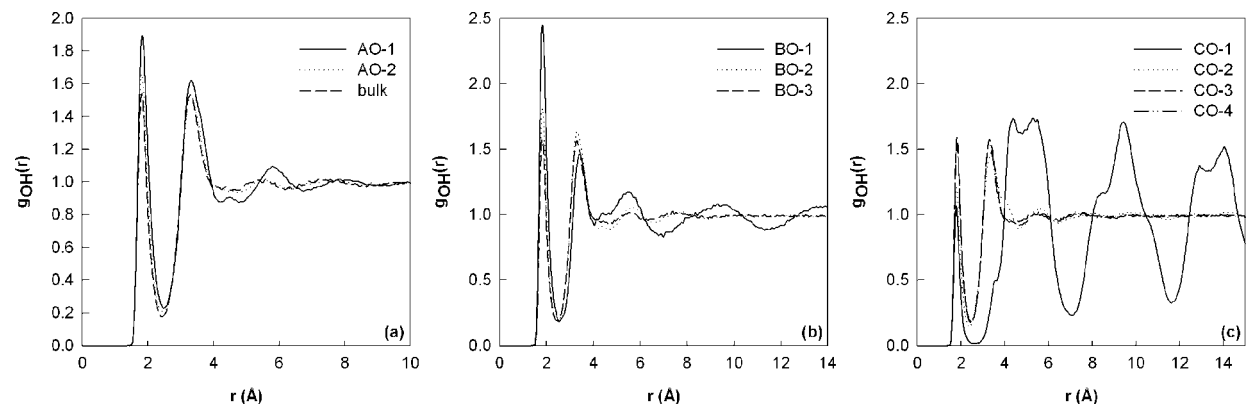


Figure 7. In-plane oxygen–hydrogen radial distribution functions $g_{OH}(r)$ on graphite (a), LD SiO₂ (b), and HD LD SiO₂ (c). The dashed line of figure (a) corresponds to a in-plane RDF far from the surfaces ($z > 14\text{Å}$) and is identical in all cases.

peaks are compared to the RDFs calculated in the center of the thin interfacial water film ($z > 14\text{Å}$), which is identified as ‘bulk’. The ‘bulk’ RDFs are identical for all surfaces considered and are only shown in panel (a) of Figure 5, Figure 6, and Figure 7. According to the RDFs, the closer the water molecules are to the surface, the more structured the fluid becomes. Upon closer inspection, the results for the in-plane RDFs demonstrate that a solid surface affects the properties of interfacial water far beyond the mere increase of density shown in Figure 4. Further, it is clear from our results that these effects are surface-specific. In the case of graphite we observe that the peaks in all the RDFs become slightly more pronounced as we move from the center of thin films to the first layer on the solid surface. However, the position of the peaks in all RDFs does not change substantially. This indicates that the structure of water near

graphite is substantially similar to that in the bulk, except for a slight increase in the density noted by previous studies and evident from the density profiles shown in Figure 4.^{41,42}

The behavior of water becomes more complex in the case of SiO₂ surfaces. Even on LD SiO₂ we note that the peaks in the RDFs change shape as well as intensity. Because the RDFs (in particular the O–H and H–H ones) are representative of the hydrogen-bonding network, these results suggest that the presence of hydroxyl groups on the SiO₂ surfaces and the atomic scale roughness affect the hydrogen-bonding network between interfacial water molecules as they approach the solid surface. This behavior becomes more extreme in the case of the HD SiO₂ surface where it is not only obvious that water molecules in the first layer cannot form hydrogen bonds between themselves (the center-to-center distance corresponding to the first

peak in layer CH-1 shifts to 5 Å, too far for hydrogen bonds to form), but they also exhibit typical features of solid-like structures. In particular the $g_{OO}(r)$ goes to zero between consecutive peaks. Because the main difference between LD and HD SiO₂ surfaces is the density of surface hydroxyl groups, it is clear that these perturb significantly the structure of water molecules, even at ambient conditions.

3.C. Structural Properties: Surface Density Distributions.

The results in Figure 5, Figure 6, and Figure 7 indicate that interesting properties of interfacial water develop near each solid surface. To further study the properties of water molecules within the first few molecular layers near a solid surface, we calculated the x-y surface density distribution of oxygen and hydrogen atoms on planes whose location corresponds to the peaks of the density profiles (see Table 2). The results should be compared to the distribution of surface hydroxyl groups for HD and LD SiO₂ shown in Figure 1. Similar to the radial distribution functions calculations, we considered slabs with thickness (δz) of 1 Å at different distances from the surface. When the calculation is performed for ‘bulk’ water at the center of the thin water film our results (not shown for brevity) indicate a uniform distribution of water molecules across the simulation box, as expected from both density profiles and in-plane RDFs discussed above. The effect of the surface on the water structure is negligible at distances larger than 14 Å from the surface for all surfaces considered.

To discuss the results we consider one surface at a time. In the case of graphite the in-plane RDFs did not indicate particular structure of interfacial water. The surface density distribution of oxygen atoms for layer AO-1 is shown in Figure 8a. The data presented in this contour plot indicate a uniform distribution of oxygen atoms in the first layer above the graphite surface. To clarify the results as well as the procedure adopted, in Figure 8b we show a drawing of the slab. The corresponding layer on the density profile is illustrated for better interpretation. A similar approach is followed in the calculations below.

In Figure 9 we provide data obtained on the LD SiO₂ surface. Panels (a) and (b) show the oxygen atom surface density profiles obtained in correspondence to peaks BO-1 and BO-2, respectively. The results presented in Figure 9a suggest a preferential distribution of oxygen atoms within layer BO-1. The high density areas of the contour plot indicate a highly structured layer where the oxygen atoms preferentially reside. The location of the high density areas is reminiscent of the hexagonal hydroxyl disposition on the solid substrate (see Figure 1a). In the second layer (BO-2), shown in Figure 9b, we observe some evidence of a preferential configuration. The oxygen atoms that belong to this layer are located approximately 1 Å above the center of the hexagons observed in layer BO-1. The presence of distinct high density areas is in agreement with the corresponding $g_{OO}(r)$. However, the features of the $g_{OO}(r)$ found on the LD SiO₂ surface are similar to the ones for the bulk water, which explains the high translational freedom of oxygen atoms suggested by the contour plots shown in Figure 9.

To complete the structural analysis in the case of water on LD SiO₂, we calculated the surface density distribution of the hydrogen atoms within specific layers. The results for hydrogen density distribution in layer BH-1 are presented in Figure 10. The data correspond to the layer located approximately 1 Å below the layer BO-1 of oxygen atoms of Figure 9a. Our results, complemented by the density profiles of Figure 4b, indicate the formation of a sparsely occupied layer where the hydrogen atoms reside along hexagonal structures. These data also suggest that water molecules in layer BO-1 form hydrogen bonds with

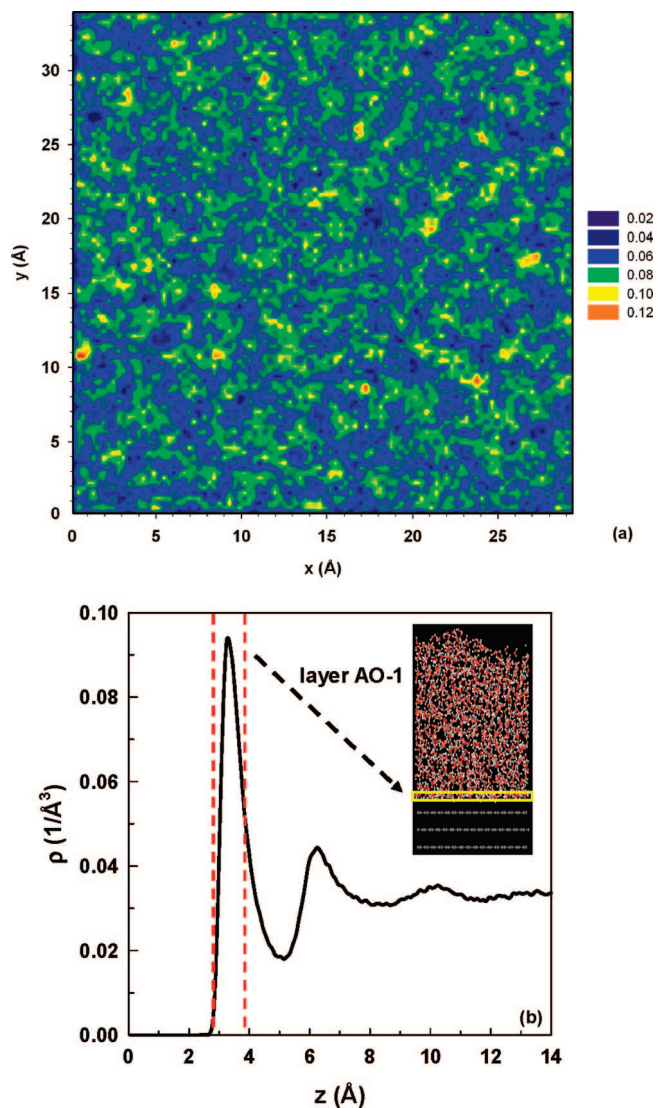


Figure 8. (a) Surface density distribution of oxygen atoms on graphite for the layer AO-1 that corresponds to the first peak of the density profile as shown schematically in panel (b). The surface density distribution is calculated on a slab of thickness 1 Å. See Table 2 for details on peak position. The units of the atomic density distribution (panel a) are Å⁻³.

those in layer BO-2. This molecular interaction may determine the distance z at which the surface manages to perturb the structure of interfacial water.

As could be expected from the RDFs results, data on the HD SiO₂ are significantly different than those on all other substrates considered above. The results are shown in Figure 11 for the surface distribution of oxygen atoms in layers CO-1 (Figure 11a) and CO-2 (Figure 11b). The results indicate that oxygen atoms in layer CO-1 adopt a well organized structure in which the oxygen atoms are highly confined within well defined areas. The high density spots are very distinct and located above the center of hexagons formed by the surface hydroxyl groups shown in Figure 1a. It should be pointed out that the distance between the high-density areas in Figure 11a corresponds to the distance between peaks in the in-plane RDFs shown in Figure 5c for layer CO-1. The pattern that appears in layer CO-2 (Figure 11b) suggests that the oxygen atoms have higher translational freedom than those in the layer CO-1. The contour plot reveals high density areas of hexagonal symmetry. The center of the hexagons observed in layer CO-2 corresponds to

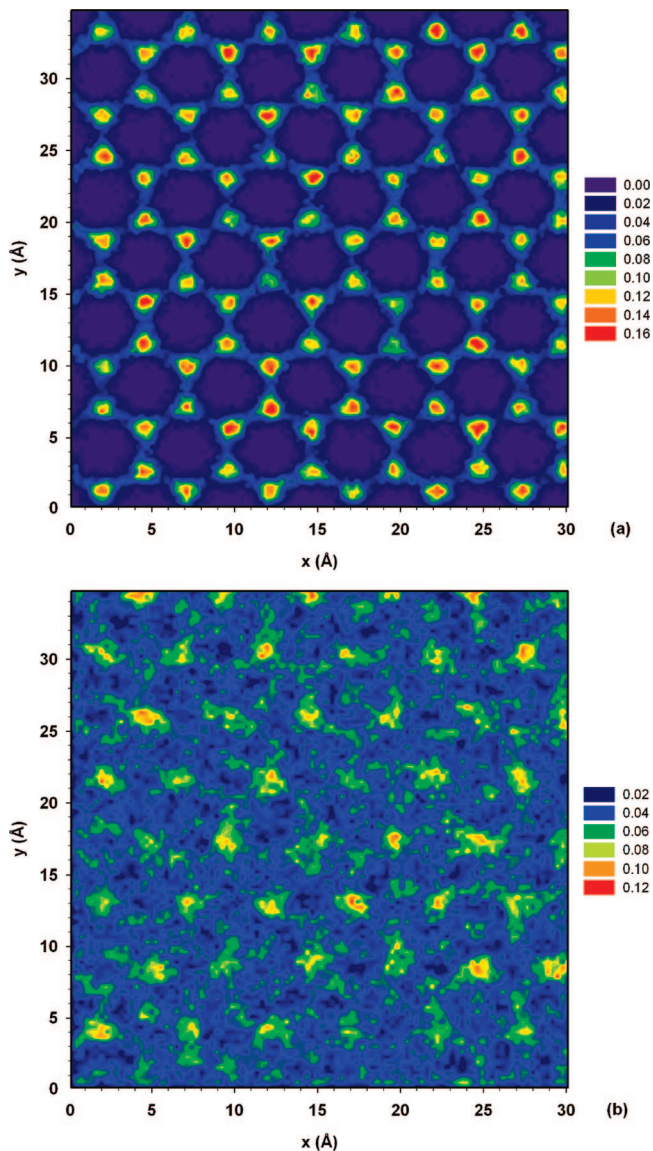


Figure 9. Surface density distribution of oxygen atoms on LD SiO₂ for the BO-1 (a) and BO-2 (b) layers. See Table 2 for details on peak position. The units of the atomic density distribution are Å⁻³.

the location of the high density areas for oxygen atoms observed in layer CO-1. However, the oxygen atoms of layer CO-2 primarily occupy every other vertex of the hexagon, and not every vertex, probably because of the establishment of a complex hydrogen-bonded network near the HD SiO₂ surface. Further, the results shown in Figure 11b suggest that all oxygen atoms located in layer CO-2 possess the ability to move along different directions in the x-y plane.

To complement the information gathered about the density distribution of oxygen atoms at the HD SiO₂ surface we report in Figure 12 the results for the surface density distribution for hydrogen atoms. Four peaks are considered: CH-1 (Figure 12a), CH-2 (Figure 12b), CH-3 (Figure 12c), and CH-4 (Figure 12d). The contour plots suggest a highly confined first layer of hydrogen atoms located 1 Å below the oxygen atoms of layer CO-1 (see Figure 12a). This finding corroborates the H-down configuration suggested by the observation of the corresponding hydrogen atomic density profiles (see Figure 4a and Figure 4b). The contour plot of Figure 12b identifies the high density areas where the hydrogen atoms exhibit preferential site occupancy in layer CH-2. This diffuse distribution of hydrogen atoms is

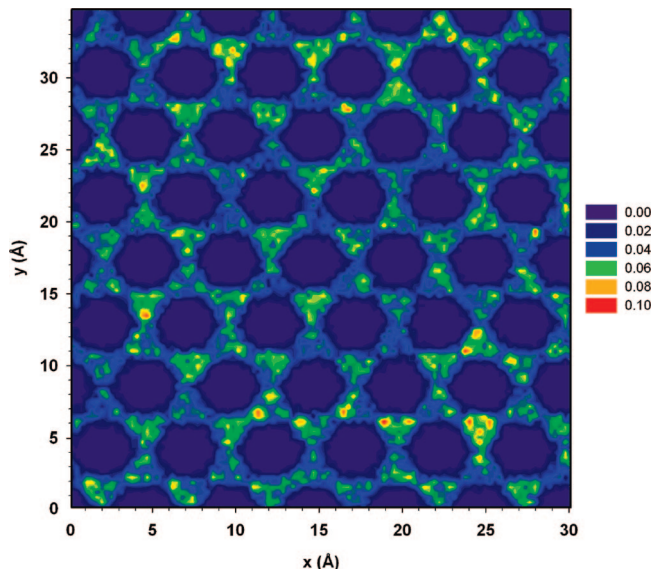


Figure 10. Surface density distribution of hydrogen atoms on BH-1 layer on LD SiO₂. See Table 2 for details on peak position. The units of the atomic density distribution are Å⁻³.

likely due to the fact that the hydrogen atoms in layer CH-2 are those covalently bonded to the oxygen atoms of layers CO-1 and CO-2. The hydrogen layer CH-2 has a higher atomic density than the hydrogen layers CH-1 and CH-3 due to the fact that it includes the hydrogen atoms of two adjacent water molecular layers. The pattern formed by the hydrogen atoms in layer CH-2 is circular and markedly different compared to the results obtained for the other layers discussed so far. The centers of the circles correspond to the position of the oxygen atoms in layer CO-1. The data analysis suggests that the first layer of water molecules is highly confined and one of the hydrogen, the one which belongs to layer CH-2, is involved in a rotational movement whose orientation is perpendicular to the surface axis formed by the second hydrogen (located in CH-1) and the oxygen (located in CO-1). The results presented in Figure 12c indicate that the hydrogen atoms within layer CH-3 are primarily located at every other vertices of a hexagonal pattern. The results shown in Figure 12a also suggest a strong limitation on translational movement for hydrogen atoms in the CH-3 layer. The results obtained in layer CH-4 (Figure 12d), located only at $z = 6.05$ Å from the HD SiO₂ surface, indicate that any sort of surface-induced pattern for hydrogen atoms vanishes at distances larger than ~ 6 Å from the surface. This latter result helps us determine at what distance the surface effect is no longer strong.

3.D. Structural Properties: Water Orientation. The density profiles in Figure 4 indicate that the surface affects the axial distribution of water molecules. Similarly, in-plane RDFs and density distributions demonstrate that the mere presence of the surface may in some cases strongly affect the structure of water, generating even solid-like structures observed in the case of water on HD SiO₂. These results are by themselves important, but for a number of applications including lubrication and for the theoretical calculation of solvation forces it is necessary to understand how the surface affects the orientation of interfacial water molecules. Thus we calculated the orientation order parameter $\langle \cos(\theta) \rangle$ of water molecules as a function of their z position. Angular brackets indicate ensemble averages. The angle θ is that between the opposite of the dipole moment vector and the vector normal to the surface. The order parameter equals zero in correspondence to an isotropic angular distribution.

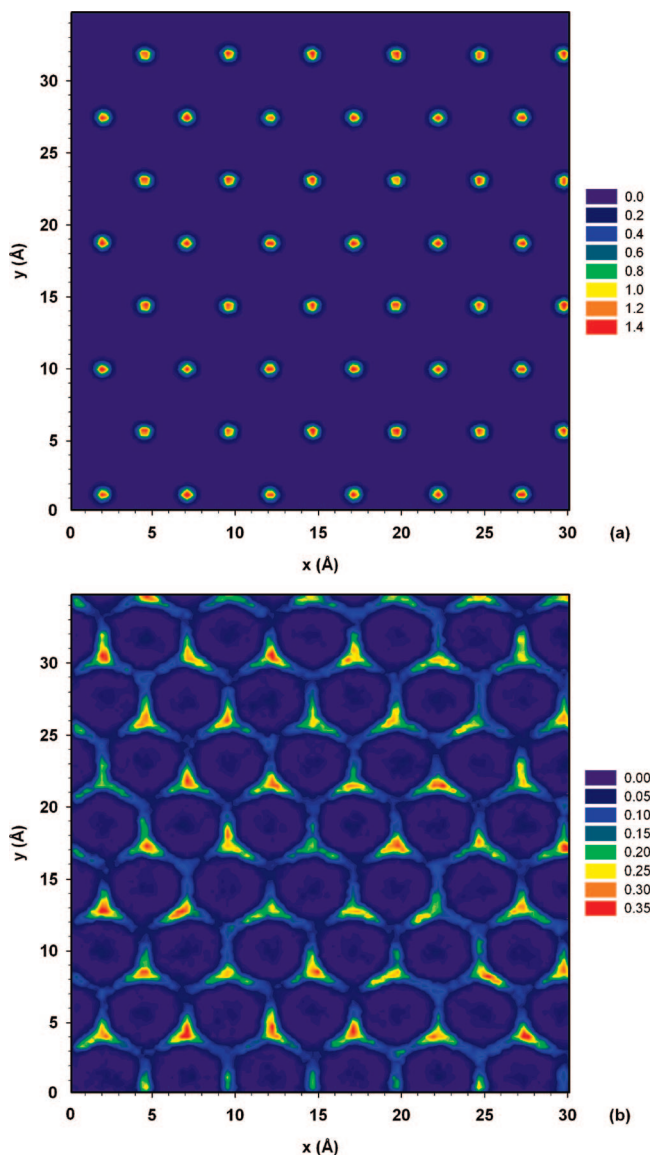


Figure 11. Surface density distribution of oxygen atoms on HD SiO₂ for the CO-1 (a) and CO-2 (b) layers. See Table 2 for details on peak position. The units of the atomic density distribution are Å⁻³.

Nonzero values indicate a preferential orientation of the water molecules. Results for the order parameter obtained at the water-vacuum interface are in agreement with those of Thomas et al.⁴³ for all surfaces considered here, and are not shown for brevity. Those obtained at the solid-water interface are shown in Figure 13. Results are only shown for values of z where water molecules are present. We observe a negative peak at approximately 2.15 Å and a positive peak at 2.85 Å for water on the HD SiO₂ surface. Similarly, we observe a negative and a positive peak for water on LD SiO₂, indicating preferential orientation of water molecules in the interfacial region. In the case of water on graphite the first broad peak that appears in Figure 13 suggests a weak preferred orientation for interfacial water molecules, as previously reported by others.^{41,42,44} According to these results, the water molecules in contact with the graphite surface tend to project some hydrogen atoms toward the solid. Although no hydrogen bonds are possible with the surface, this configuration is thought to maximize the number of water–water hydrogen bonds.

A more detailed picture of the orientation of interfacial water molecules is provided by the results presented in Figure 14 and

Figure 15 where the time average of the angle θ is shown within x - y planes at specific distances from the solid surface. In Figure 14 we show results for water on LD SiO₂ surface corresponding to layers BO-1 (Figure 14a) and BO-2 (Figure 14b). The data in Figure 14a suggest a hydrogen-down orientation for the water molecules in layer BO-1 that occurs in hexagonal patterns around the surface hydroxyl groups. These results should be interpreted in the context of the corresponding density contour plots. By doing so we conclude that water molecules that belong to the high density areas shown in Figure 9a have an average θ value of approximately 120°. However, when water molecules approach a surface hydroxyl group the angle decreases (light blue areas) because of a change in the orientation. A pattern similar to that obtained for layer BO-1 is observed within the layer BO-2 (Figure 14b) with the difference that the regions with large oxygen densities that are characterized by small θ . When water molecules migrate to the region of low oxygen density the orientation changes and the angle increases.

The results obtained in the first layer (CO-1) on the HD SiO₂ surface, shown in Figure 15a, indicate a well defined orientation for the interfacial water molecules. The oxygen atoms in this layer are highly confined and water molecules highly oriented with an average angle θ of approximately 120°. This finding corroborates the preferred hydrogen-down orientation observed for water molecules near the solid HD SiO₂ surface. According to the results in the same figure, water molecules maintain the same orientation even when they leave (not by much) the high density areas. The results also indicate that the angle θ is $\sim 50^\circ$ when water molecules occupy low density areas. Similarly in Figure 15b a small angle θ ($<80^\circ$) is observed in correspondence to the high density regions of the oxygen layer CO-2. The orientation changes significantly when water molecules occupy the low density regions, θ increases above 80°, and in some cases reaches 120°. Similar calculations (not shown for brevity) were conducted for the graphite surface, but only a limited degree of preferential orientation was observed in the first two interfacial layers in agreement with all the data reported above. All the above results illustrate the impact of the substrate on the structural properties of water in the interfacial region. Significant and more pronounced are the effects on the water orientation on the HD SiO₂ surface. The large surface density of hydroxyl groups on this surface allows water molecules to adsorb in an organized manner within the first few molecular layers away from the surface. In the case of LD SiO₂ and graphite the surface effects are less pronounced and a lower degree of orientation is observed.

3.E. Structural Properties: Hydrogen Bonding. The results of the planar density profiles and orientation of water molecules suggest that the presence of a solid surface directly affects interfacial water. This behavior may lead to the formation of an extended and fairly stable hydrogen-bonded network away from the surface. We calculated the average numbers of hydrogen bonds established between water molecules as a function of distance from the surface. To define a hydrogen bond we used the geometric criterion proposed by Martí.⁴⁵ The position of the hydrogen bond was defined as that of the mid distance between the hydrogen of the donor and the oxygen of the acceptor molecules. The results are shown in Figure 16 in terms of the density of hydrogen bonds as a function of the distance z from the solid surface. The data indicate increased density of hydrogen bonds at specific distances from the three surfaces. In the case of graphite and LD SiO₂, the hydrogen bond density peaks are located at approximately 3.45 and 3.00 Å, respectively, which approximately correspond to the peaks

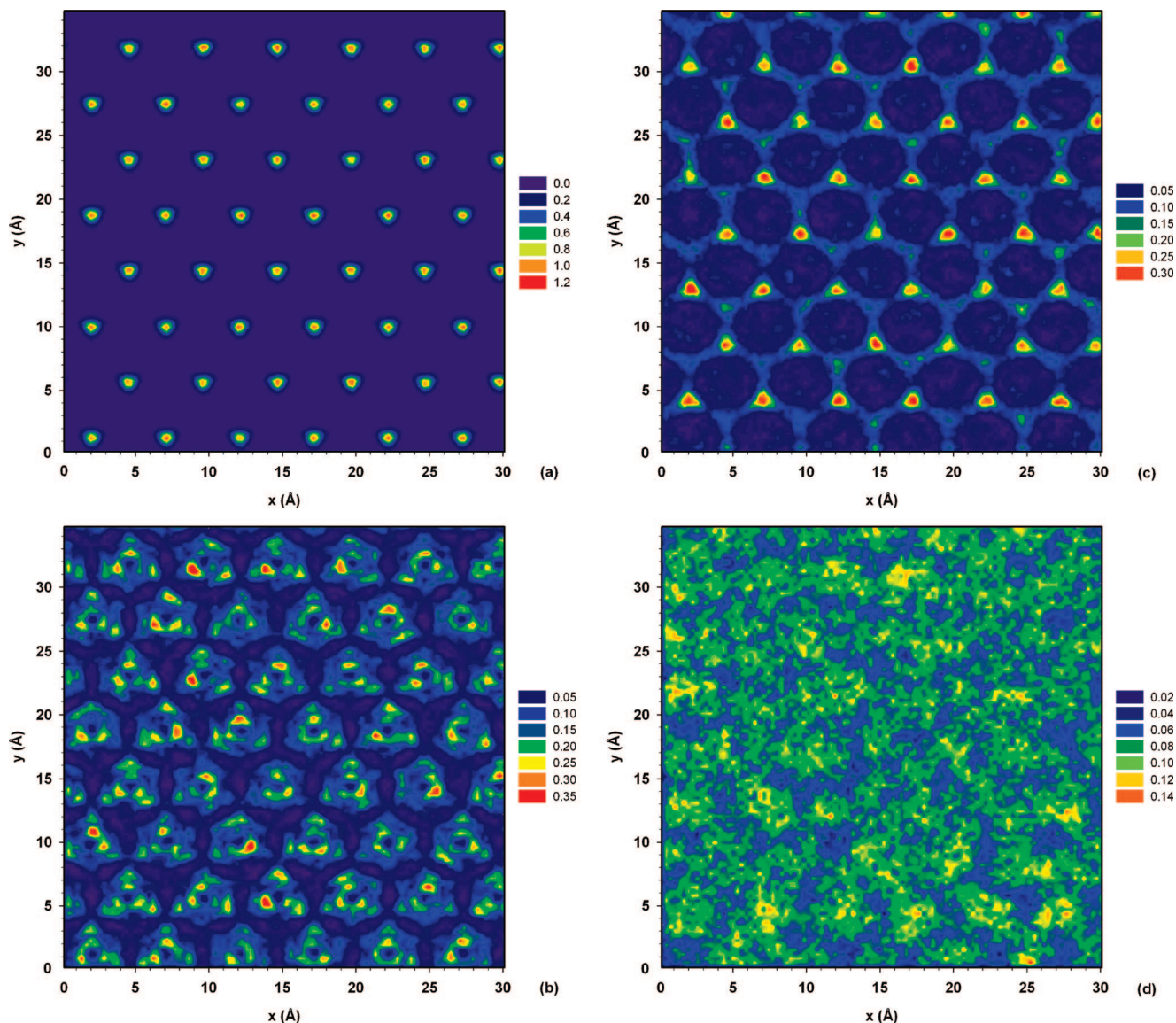


Figure 12. Surface density distribution of hydrogen atoms for the CH-1 (a), CH-2 (b), CH-3 (c), and CH-4 (d) layers on HD SiO₂. See Table 2 for details on peak position. The units of the atomic density distribution are Å⁻³.

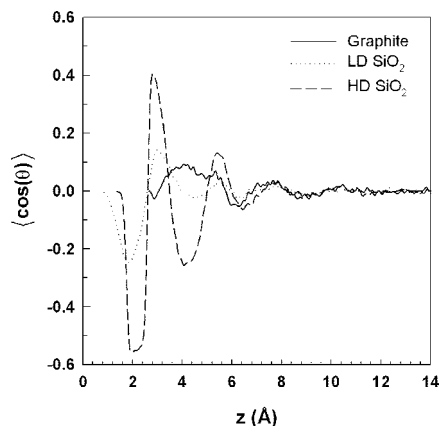


Figure 13. Order parameter $\langle \cos(\theta) \rangle$ for water molecules as a function of their distance from the surface. The angle θ is that between the opposite to the dipole moment vector of water and the normal to the surface vector.

of the oxygen atomic density profiles. This suggests that the large number of water molecules in the first layers form hydrogen bonds among themselves. The bonding environment

of water on the HD SiO₂ surface is remarkably different. In this case a high hydrogen bond density is located at ~ 2.65 Å, which corresponds to the region in between two oxygen layers (CO-1 and CO-2). This indicates that the formation and structural behavior of the second molecular layer is highly dependent on the hydrogen bond network. The highly confined water molecules of the first layer cannot establish hydrogen bonds between themselves. As a result they form hydrogen bonds with the water molecules of the second molecular layer, highly affecting their configuration. Compelling evidence of this is presented in Figure 16b where the in-plane hydrogen bond density distribution that corresponds to the first peak of Figure 16a for water on the HD SiO₂ is shown as a function of the x and y direction. It is worth noting that the hydrogen bonds are located in specific positions and that these positions are in between the peaks of oxygen atom in the x - y plane obtained in correspondence to the peak CO-1 and CO-2 (see Figure 4a, Figure 11a, and Figure 11b).

3.F. Dynamic Properties: Residence Correlation Functions. The equilibrium properties discussed so far indicate that the surface, especially in the case of HD SiO₂, can profoundly affect the structure of interfacial water. It is also of interest to

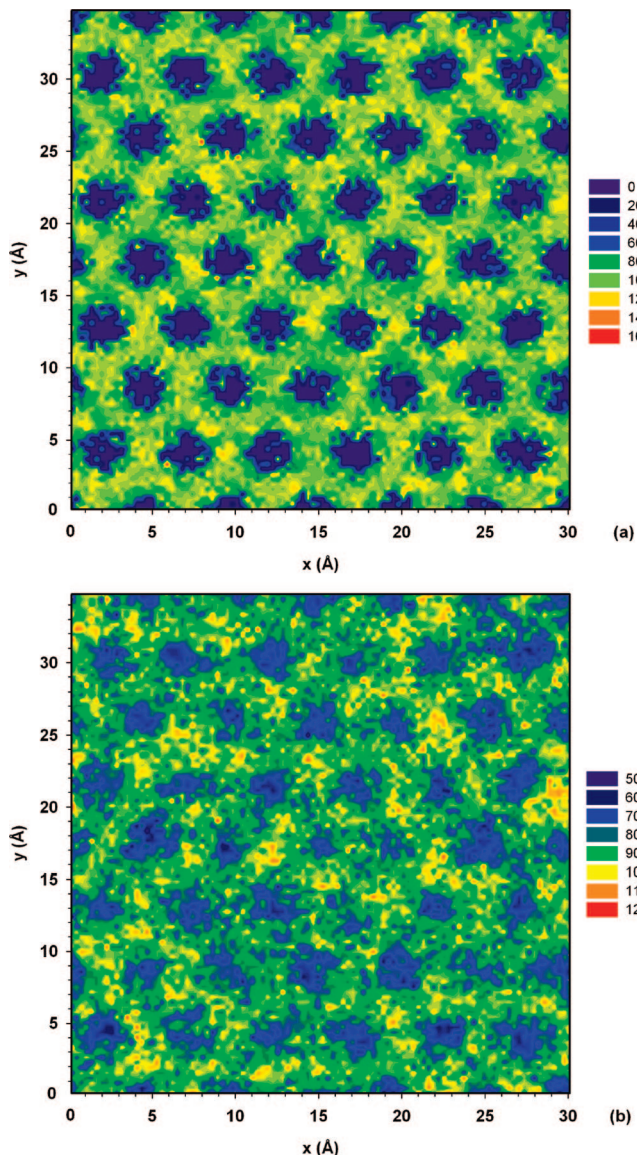


Figure 14. Contour plots showing the water orientation for water layers BO-1 (a) and BO-2 (b) on the LD SiO₂ surface. The average values of the angle θ between the vector opposite to the dipole moment of water and that normal to the surface are plotted with respect to the x and y positions. See Table 2 for details on peak position. The angle θ is in degrees.

understand the residence times of water molecules within the layers and their exchange rate with those in the bulk. A residence correlation function $C_R(t)$ was employed to study the residence time of the water molecules in specific layers of interest. In each case a slab of thickness 1 Å was considered in correspondence to the peaks that appear in Figure 4a (see Table 2 for peak position). The residence correlation function is then calculated as

$$C_R(t) = \frac{\langle O_w(t)O_w(0) \rangle}{\langle O_w(0)O_w(0) \rangle} \quad (1)$$

where angular brackets designate ensemble averages. The term $O_w(t)$ describes whether an oxygen atom is, or is not, in the slab of interest at time t . The values for $O_w(t)$ are 1 or 0 when an atom belongs to the layer or not, respectively. The correlation function is expected to decay from 1 to 0 as time progresses in response to the movement of water molecules in and out of a specific layer. The more slowly the correlation function

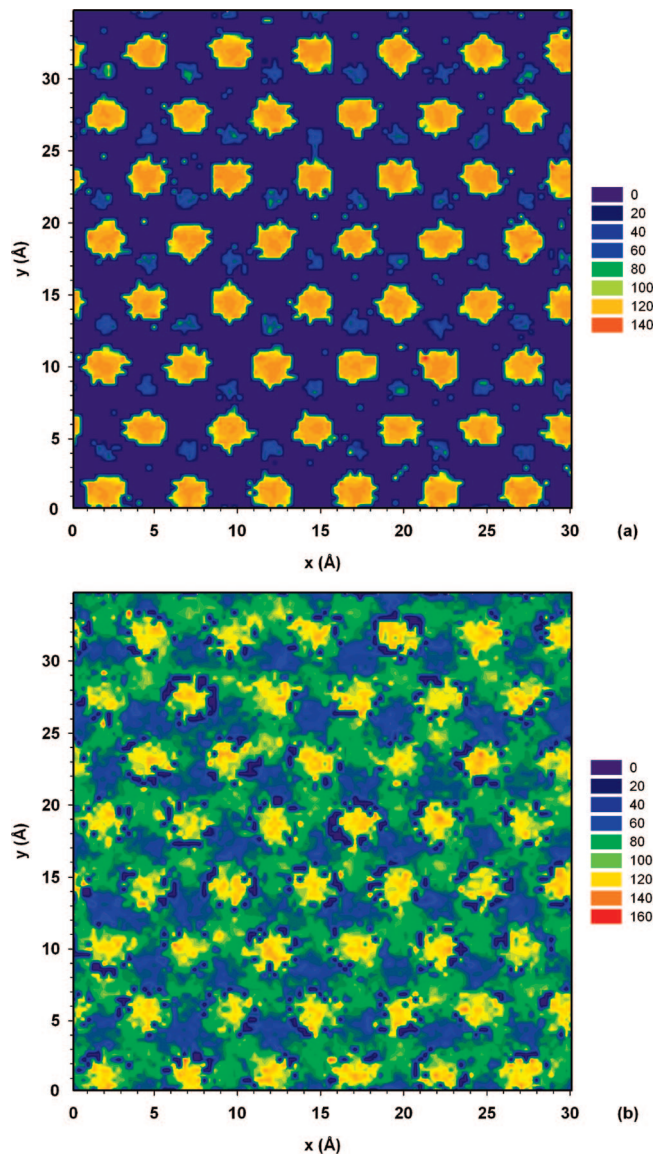


Figure 15. Same as Figure 14. The angle θ is calculated for water molecules on the HD SiO₂ surface for the oxygen layer CO-1 (a) and CO-2 (b). See Table 2 for details on peak position. The angle θ is in degrees.

decreases, the longer the water molecules remain in the slab being examined. For example, based on the results shown in Figure 17a water molecules in the layer AO-1 on graphite remain longer in that layer than those in the AO-2 layer. The results regarding bulk water ($z > 14$ Å) are identical for all three surfaces, further indicating that there is no impact of the surface on any of the water properties at that separation. In all cases, the autocorrelation function of the bulk decreases faster than any other calculated autocorrelation function.

The results presented in Figure 17 suggest that for most cases the water molecules close to the surface have the tendency to remain longer in that region compared to molecules found further from the surface. A different behavior is observed for water on LD SiO₂, in which case our results show that the residence time of water molecules in the layer BO-1 is not as long as in the denser layer BO-2. We ascribe this counter-intuitive result to the fact that the layer BO-1 is not really separated from the layer BO-2 (it corresponds to a shoulder in the density profiles of Figure 4). Thus water molecules are relatively free to leave the layer BO-1. The dynamic behavior

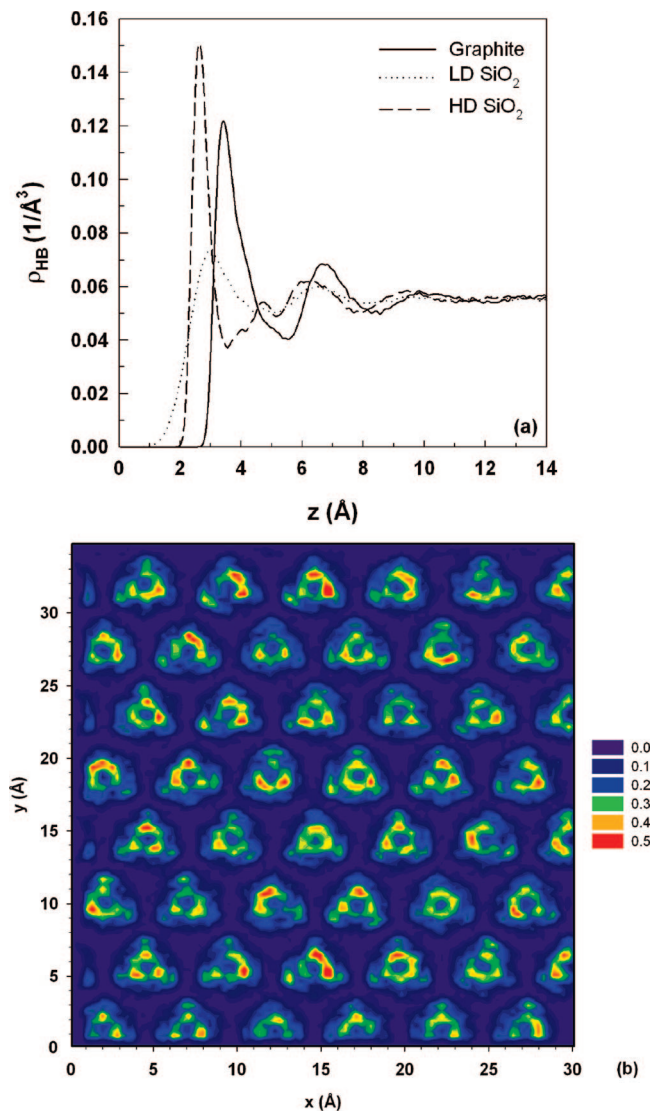


Figure 16. (a) Density profiles of the hydrogen bonds formed between water molecules as a function of distance from the solid surface. (b) Hydrogen bond surface density distribution correspondent to the first peak found for water on HD SiO₂, as shown in Figure 16a. Units in Figure 16b are \AA^{-3} .

TABLE 3: Time Required for the Autocorrelation Function to Decay from 1 to 1/e for All Layers on the Different Surfaces Considered^a

substrate	layer	time (ps)
graphite	AO-1	34.9 ± 0.6
	AO-2	3.9 ± 0.2
LD SiO ₂	BO-1 ^b	4.7 ± 0.1
	BO-2	6.8 ± 0.2
	BO-3	2.4 ± 0.1
HD SiO ₂	CO-1	237.3 ± 33.4
	CO-2	45.1 ± 1.0
	CO-3	5.8 ± 0.2
bulk (any substrate at $z > 14$ \AA)	bulk	1.65 ± 0.02

^a Results are obtained from the ACFs shown in Figure 17. ^b This layer corresponds to a shoulder in the density profile.

of water molecules at the HD SiO₂ surface is quantified in Figure 17c. The oxygen atoms of the first layer (CO-1) at the HD SiO₂ surface are highly confined, as suggested by the surface density distribution. In agreement with those calculations are the results of the correlation function that clearly indicate a significant residence time in the first interfacial layer. For the same system

the results suggest a relatively long residence time in the second layer (CO-2) compared to water molecules on graphite and on LD SiO₂. This also suggests a limited exchange of water molecules between the first and the second molecular layers formed on HD SiO₂. Thus the restricted movement of the first layer molecules at HD SiO₂ in the x and y directions suggested by the contour plot of Figure 11a, is coupled to a slow exchange rate with bulk water molecules in the z direction.

To quantify these qualitative observations we calculated the residence time as the time required for the autocorrelation function to decay from 1 to 1/e for all the cases considered in Figure 17. The results are presented in Table 3. We observe a significant difference between the residence times on the layer CO-1 on HD SiO₂ (~ 237.3 ps) compared to that in bulk water (~ 1.7 ps). It is also important to point out that the residence time for water in the first layer on graphite is significantly larger than that obtained in any of the three layers considered on LD SiO₂. This latter result is quite surprising when we consider that graphite cannot establish hydrogen bonds with interfacial water molecules, and it is probably due to longer-lasting water–water hydrogen bonds formed at the water–graphite interface.

3.G. Dynamic Properties: Reorientation Correlation Functions. Another dynamic quantity of interest is the frequency by which water molecules change their orientation as a function of the distance from each of the solid substrates. To assess this property, we computed reorientation autocorrelation functions for water molecules corresponding to different layers on the three substrates. In each case, we selected a slab of thickness 1 \AA correspondent to the peaks in Figure 4a (see Table 2 for peak position). The reorientation of two vectors, defined by the geometry of a water molecule, was considered. The first vector is the opposite of the molecular dipole moment of one water molecule (\underline{DM}) and the second is the hydrogen–hydrogen vector (\underline{HH}). Each reorientation autocorrelation function was calculated as:

$$C_{\mu}(t) = \frac{\langle \hat{\mu}(t) \hat{\mu}(0) \rangle}{\langle \hat{\mu}(0) \hat{\mu}(0) \rangle} \quad (2)$$

where angular brackets designate ensemble averages. The symbol $\hat{\mu}$ represents the \underline{DM} and \underline{HH} unit vectors in each case. The corresponding correlation functions, $C_{DM}(t)$ and $C_{HH}(t)$, are shown in Figures 18 and 19, respectively. Panels a–c are results obtained on graphite, LD SiO₂, and HD SiO₂, respectively.

The results can be compared to those obtained for bulk water (panel a in both Figure 18 and Figure 19). Both bulk reorientation autocorrelation functions show fast decay from 1 to 0, and the two data sets do not differ. This indicates that the rotation of bulk water molecules is isotropic. Because the results for bulk water do not depend on the surface, we again conclude that surface effects do not extend to 14 \AA from the solid substrates under consideration. The results for the reorientation autocorrelation function for water in the various layers formed on the three substrates follow the general trend observed for the residence autocorrelation function of Figure 17. Namely, the closer a layer is to the solid surface, the slower the reorientation of the water molecules that belong to that layer. An exception, as in the case for the residence autocorrelation function, is observed in the case of water on LD SiO₂. In this case, the reorientation in layer BO-2 is the slowest of the three layers considered, whereas the reorientation in layer BO-1 is almost as fast as that observed in layer BO-2. In general, the reorientation autocorrelation function of the \underline{DM} vector is slower than

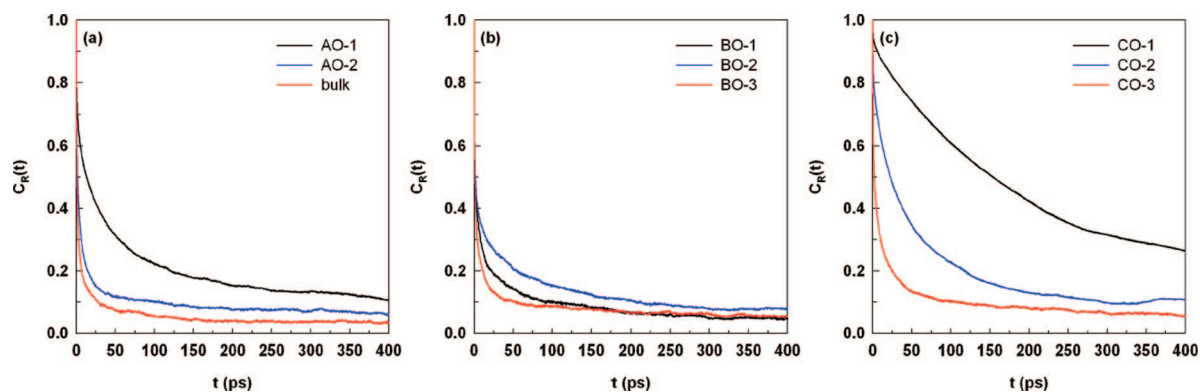


Figure 17. Residence correlation functions for oxygen atoms in the various layers at the graphite (a), LD SiO₂ (b), and HD SiO₂ (c) surfaces. See Table 2 for details on peak position.

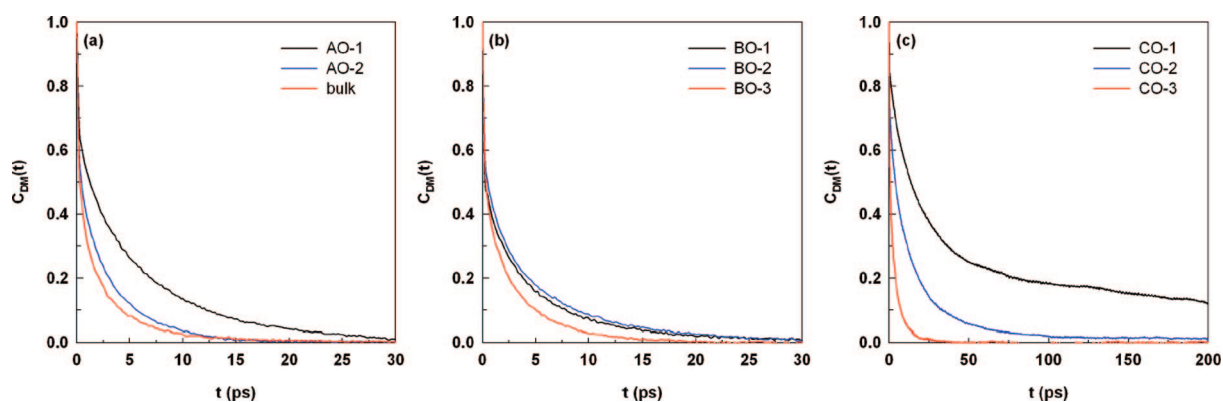


Figure 18. Reorientation autocorrelation function for the vector opposite to the molecular dipole moment of water. Results are shown in correspondence to various layers at the graphite (a), LD SiO₂ (b), and HD SiO₂ (c) surfaces. See Table 2 for details on peak position.

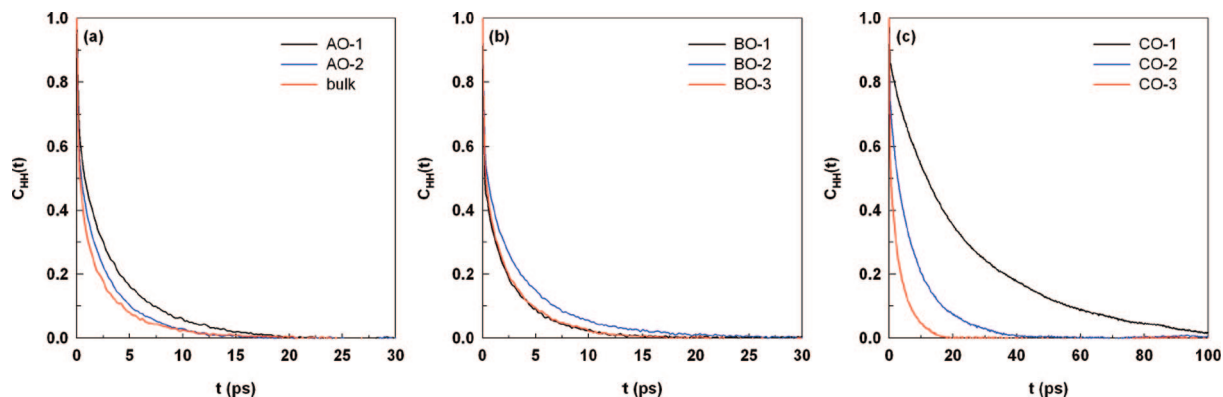


Figure 19. Reorientation autocorrelation function for the hydrogen–hydrogen vector of water. Results are shown in correspondence to various layers at the graphite (a), LD SiO₂ (b), and HD SiO₂ (c) surfaces. See Table 2 for details on peak position.

that of \overrightarrow{HH} , suggesting that the presence of solid substrate determines anisotropic rotation of interfacial water molecules. The effect is very pronounced for water molecules in layer CO-1 on HD SiO₂. This observation is probably due to the fact that solid–water interactions determine, for the most part, the orientation of the \overrightarrow{DM} of those water molecules at contact with the HD SiO₂. The \overrightarrow{HH} orientation may be primarily determined by water–water hydrogen bonds, which can fluctuate rapidly.

4. Conclusions

We investigated structural and dynamic properties of water molecules within the first few molecular layers in contact with three solid surfaces. The surfaces (graphite and two SiO₂ substrates) were chosen to assess the effects of different

degrees of hydrophobicity. In order to study the structural properties we calculated atomic density profiles, in-plane radial distribution functions, in-plane density distributions, preferential orientations, and hydrogen-bond density profiles. Our results confirm that the solid substrate perturbs interfacial water molecules for only a few molecular diameters away from the surface. In the case of graphite and SiO₂ with low density of hydroxyl groups, the interfacial water shows increased density compared to the bulk. When the density of hydroxyl groups increases, we observe the formation of a highly ordered contact layer and that of a second dense layer. The detailed analysis of the equilibrated structure revealed important results concerning the structure of the interfacial water molecules. Most significant are the results for the hydrogen bond network within the interfacial layers. These

suggest that the properties of the second layer are determined by the water–water hydrogen bonds formed with the water molecules in the first layer.

Dynamic properties were assessed by calculating residence and reorientation autocorrelation functions for water as a function of the distance from the solid substrates. Our results suggest a longer residence time for the water molecules found on the first layer on SiO₂ surface with high density of hydroxyl groups compared to all other cases. Results for the reorientation autocorrelation function follow trends similar to those observed for the residence autocorrelation function, suggesting that as the water molecules reside longer in specific locations close to the surface they also rotate less freely. In addition, we found evidence for anisotropic reorientation autocorrelation function. Namely, the vector identified by the two hydrogen atoms of a water molecule reorients significantly faster than the vector opposite to the water dipole moment. This behavior is particularly evident in the case of water in contact with HD SiO₂ surfaces. Our results also indicate that the dynamic behavior computed at 14 Å away from any surface is isotropic and identical for all three surfaces, further suggesting that there is no impact by the substrate on any of the water properties at distances larger than a few molecular diameters. The data presented here suggest that not only the solid surface, but also preferential interaction between interfacial water molecules may result in macroscopic phenomena typically used to discriminate between hydrophobic and hydrophilic surfaces. These new results provide a fundamental basis for investigating, in more detail, the molecular-scale phenomena relevant to nanofluidics and other nanotechnological applications.

Acknowledgment. Financial support was provided, in part, by the U.S. Department of Energy through funding provided by the Divisions of Materials Sciences and Engineering and Chemical Sciences, Geosciences and Biosciences, Office of Basic Energy Sciences, U.S. Department of Energy, by Contract No. DE-AC05-00OR22725 to Oak Ridge National Laboratory (managed and operated by UT-Battelle, LLC). D.A., N.R.T., and A.S. acknowledge partial financial support from the Oklahoma State Regents for Higher Education. Generous allocations of computing time were provided by the OU Supercomputing Center for Education and Research (OSCCER) at the University of Oklahoma and by the National Energy Research Scientific Computing Center (NERSC) at Lawrence Berkeley National Laboratory.

References and Notes

- (1) Barrer, R. M. *Zeolites and Clay Minerals as Sorbents and Molecular Sieves*; Academic Press: London, 1978.
- (2) Hensen, E. J. M.; Smit, B. *J. Phys. Chem. B* **2002**, *106*, 12664.
- (3) Bhushan, B.; Israelachvili, J. N.; Landman, U. *Nature* **1995**, *374*, 607.
- (4) Leng, Y.; Cummings, P. T. *Phys. Rev. Lett.* **2005**, *94*, 026101.
- (5) Binggeli, M.; Mate, C. M. *Appl. Phys. Lett.* **1994**, *65*, 415.
- (6) Darhuber, A. A.; Troian, S. M. *Ann. Rev. Fluid Mechanics* **2005**, *37*, 425.
- (7) Craighead, H. *Nature* **2006**, *442*, 387.
- (8) Srinivasan, V.; Pamula, V. K.; Fair, R. B. *Lab Chip* **2004**, *4*, 310.
- (9) Pal, S. K.; Zewail, A. H. *Chem. Rev.* **2004**, *104*, 2099.
- (10) Tajkhorshid, E.; Nollert, P.; Jensen, M. O.; Miercke, L. J. W.; O'Connell, J.; Stroud, R. M.; Schulten, K. *Science* **2002**, *296*, 525.
- (11) Hille, B. *Ionic channels in excitable membranes*; Sinauer Associates: Sunderland, MA, 1992.
- (12) Cox, J. J.; Reimann, F.; Nicholas, A. K.; Thornton, G.; Roberts, E.; Springell, K.; Karbani, G.; Jafri, H.; Mannan, J.; Raashid, Y.; Al-Gazali, L.; Hamamy, H.; Valente, E. M.; Gorman, S.; Williams, R.; McHale, D. P.; Wood, J. N.; Gribble, F. M.; Woods, C. G. *Nature* **2006**, *444*, 894.
- (13) Fitter, J.; Lechner, R. E.; Dencher, N. A. *J. Phys. Chem. B* **1999**, *103*, 8036.
- (14) Kim, J.; Lu, W.; Qiu, W.; Wang, L.; Caffrey, M.; Zhong, D. *J. Phys. Chem. B* **2006**, *110*, 21994.
- (15) Israelachvili, J.; Pashley, R. *Nature* **1982**, *300*, 341.
- (16) Mamontov, E.; Vlcek, L.; Wesolowski, D. J.; Cummings, P. T.; Wang, W.; Anovitz, L. M.; Rosenqvist, J.; Brown, C. M.; GarciaSakai, V. *J. Phys. Chem. C* **2007**, *111*, 4328.
- (17) Bruni, F.; Ricci, M. A.; Soper, A. K. *J. Chem. Phys.* **1998**, *109*, 1478.
- (18) Puibasset, J.; Pellenq, R. J. M. *J. Chem. Phys.* **2003**, *119*, 9226.
- (19) Lee, S. H.; Rosky, P. J. *J. Chem. Phys.* **1994**, *100*, 3334.
- (20) Gallo, P.; Ricci, M. A.; Rovere, M. *J. Chem. Phys.* **2002**, *116*, 342.
- (21) Gordillo, M. C.; Nagy, G.; Martí, J. *J. Chem. Phys.* **2005**, *123*, 054707.
- (22) Leng, Y.; Cummings, P. T. *J. Chem. Phys.* **2006**, *124*, 074711.
- (23) Giovambattista, N.; Debenedetti, P. G.; Rosky, P. J. *J. Phys. Chem. C* **2007**, *111*, 1323.
- (24) Nangia, S.; Washton, N. M.; Mueller, K. T.; Kubicki, J. D.; Garrison, B. J. *J. Phys. Chem. C* **2007**, *111*, 5169.
- (25) Janeczek, J.; Netz, R. R. *Langmuir* **2007**, *23*, 8417.
- (26) Gordillo, M. C.; Martí, J. *J. Chem. Phys.* **2002**, *117*, 3425.
- (27) Spohr, E. *J. Chem. Phys.* **1997**, *106*, 388.
- (28) Weiss, D. R.; Raschke, T. M.; Levitt, M. *J. Phys. Chem. B* **2008**, *112*, 2981.
- (29) Gordillo, M. C.; Martí, J. *Chem. Phys. Lett.* **2000**, *329*, 341.
- (30) Gordillo, M. C.; Martí, J. *Phys. Rev. B* **2003**, *67*, 205425.
- (31) Striolo, A. *Nano Lett.* **2006**, *6*, 633.
- (32) Striolo, A.; Chialvo, A. A.; Gubbins, K. E.; Cummings, P. T. *J. Chem. Phys.* **2005**, *122*, 234712.
- (33) Verdager, A.; Sacha, G. M.; Bluhm, H.; Salmeron, M. *Chem. Rev.* **2006**, *106*, 1478.
- (34) Schmahl, W. W.; Swainson, I. P.; Dove, M. T.; Graeme-Barber, A. Z. *Kristallogr.* **1992**, *201*, 125.
- (35) Berendsen, H. J. C.; Grigera, J. R.; Straatsma, T. P. *J. Phys. Chem.* **1987**, *91*, 6269.
- (36) Cheng, A.; Steele, W. A. *J. Chem. Phys.* **1990**, *92*, 3858.
- (37) Brodka, A.; Zerda, T. W. *J. Chem. Phys.* **1996**, *104*, 6319.
- (38) Allen, M. P.; Tildesley, D. J. *Computer Simulation of Liquids*; Oxford University Press: Oxford, 2004.
- (39) Ryckaert, J.-P.; Ciccotti, G.; Berendsen, H. J. C. *J. Comput. Phys.* **1977**, *23*, 327.
- (40) Plimpton, S. *J. Comput. Phys.* **1995**, *117*, 1.
- (41) Martí, J.; Nagy, G.; Gordillo, M. C.; Guardia, E. *J. Chem. Phys.* **2006**, *124*, 094703.
- (42) Striolo, A.; Chialvo, A. A.; Cummings, P. T.; Gubbins, K. E. *Langmuir* **2003**, *19*, 8583.
- (43) Thomas, J. L.; Roesselova, M.; Dang, L. X.; Tobias, D. J. *J. Phys. Chem. A* **2007**, *111*, 3091.
- (44) Pertsin, A.; Grunze, M. *J. Phys. Chem. B* **2004**, *108*, 1357.
- (45) Martí, J. *J. Chem. Phys.* **1999**, *110*, 6876.